www.nature.com/aps

Acta Pharmacologica Sinica

ARTICLE

The C terminus of DJ-1 determines its homodimerization, MGO detoxification activity and suppression of ferroptosis

Li Jiang[1], Xiao-bing Chen[1], Qian Wu[1], Hai-ying Zhu[1], Cheng-yong Du[2], Mei-dan Ying[1], Qiao-jun He[1,3,4], Hong Zhu[1], Bo Yang[1] and Ji Cao[1,3,4]

DJ-1 is a multifunctional protein associated with cancers and autosomal early-onset Parkinson disease. Besides the well-documented antioxidative stress activity, recent studies show that DJ-1 has deglycation enzymatic activity and anti-ferroptosis effect. It has been shown that DJ-1 forms the homodimerization, which dictates its antioxidative stress activity. In this study, we investigated the relationship between the dimeric structure of DJ-1 and its newly reported activities. In HEK293T cells with Flag-tagged and Myc-tagged DJ-1 overexpression, we performed deletion mutations and point mutations, narrowed down the most critical motif at the C terminus. We found that the deletion mutation of the last three amino acids at the C terminus of DJ-1 (DJ-1 ΔC3) disrupted its homodimerization with the hydrophobic L187 residue being of great importance for DJ-1 homodimerization. In addition, the ability in methylglyoxal (MGO) detoxification and deglycation was almost abolished in the mutation of DJ-1 ΔC3 and point mutant L187E compared with wild-type DJ-1 (DJ-1 WT). We also showed the suppression of erastin-triggered ferroptosis in DJ-1$^{-/-}$ mouse embryonic fibroblast cells was abolished by ΔC3 and L187E, but partially diminished by V51C. Thus, our results demonstrate that the C terminus of DJ-1 is crucial for its homodimerization, deglycation activity, and suppression of ferroptosis.

Keywords: DJ-1; C terminus; homodimerization; methylglyoxal (MGO) detoxification; deglycation; ferroptosis; HEK293T cells; DJ-1$^{-/-}$ mouse embryonic fibroblast cells

Acta Pharmacologica Sinica (2021) 42:1150–1159; https://doi.org/10.1038/s41401-020-00531-1

INTRODUCTION

DJ-1 is a highly conserved multifunctional protein first identified as an oncogene synergistically transforming mouse NIH3T3 cells with activated GTPase HRas (HRAS) and MYC proto-oncogene (c-Myc) [1]. It is localized predominantly in the cytoplasm and partially in the mitochondria, and it is also expressed in the nucleus of several cell types [1–3]. It has been reported that DJ-1 is overexpressed in multiple tumor cells and is positively related to tumor metastasis and poor prognosis for patients, which further suggests that it is a potential predictive biomarker for cancer diagnosis and prognosis [4–6]. Moreover, knocking down DJ-1 promotes the efficacy of chemotherapeutic drugs in some tumor cells [7]. The regulatory mechanism of oncogenic transformation by DJ-1 is reported to be associated with the inactivation of phosphatase and tensin homolog (PTEN) and activation of the Raf-1 proto-oncogene serine/threonine kinase (c-Raf) [8, 9]. In addition, the well-known effects of DJ-1 on antioxidative stress might be essential for tumorigenesis and cancer progression [7, 10]. DJ-1 undergoes irreversible oxidation at the Cys106 residue to directly eliminate reactive oxygen species (ROS) [11–17]. Mechanistically, the role of DJ-1 as an abundant antioxidant scavenger of soluble ROS (such as H_2O_2) is related to the antioxidant transcriptional master regulator nuclear factor erythroid 2-related factor 2 (NRF2), which orchestrates the expression of genes coding stress response and antioxidant proteins [10, 18]. In addition, we have shown that DJ-1 functions as a key factor protecting tumor cells by affecting both soluble ROS and lipid ROS with distinct mechanisms [19, 20]. The different oxidation states of DJ-1 determine cell fate either by activating autophagy or apoptosis through the regulation of apoptotic signal-regulating kinase 1 (ASK1) activity, which is affected through the activity of DJ-1 against soluble ROS [20]. Most recently, DJ-1 was shown to suppress ferroptosis triggered by lipid ROS by maintaining the level of cysteine synthesized in the transsulfuration pathway, the predominant source of cysteine for glutathione (GSH) biosynthesis when the cystine/glutamate transporter (SLC7A11, xCT) is inhibited [19]. Notably, the suppression of DJ-1 expression dramatically enhanced the sensitivity of tumor cells both in vitro and in vivo to the ferroptosis inducer erastin [19]. Thus, DJ-1 is further proposed as a potential therapeutic target for cancer therapy.

Although DJ-1 was initially reported as an antioxidative enzyme by directly reducing mixed disulfides in covalently modified proteins, some evidence has also suggested that DJ-1 has chaperone activity and can be converted from a zymogen to a protease by carboxyl-terminal cleavage [15, 21–24]. Interestingly,

[1]Institute of Pharmacology and Toxicology, Zhejiang Province Key Laboratory of Anti-Cancer Drug Research, College of Pharmaceutical Sciences, Zhejiang University, Hangzhou 310058, China; [2]Department of Breast Surgery, The First Affiliated Hospital, College of Medicine, Zhejiang University, Hangzhou 310006, China; [3]Innovation Institute for Artificial Intelligence in Medicine, Zhejiang University, Hangzhou 310058, China and [4]Cancer center of Zhejiang University, Hangzhou 310058, China
Correspondence: Ji Cao (caoji88@zju.edu.cn)
These authors contributed equally: Li Jiang, Xiao-bing Chen

Received: 8 March 2020 Accepted: 7 September 2020
Published online: 6 October 2020

recent studies have shown DJ-1 exhibits glyoxalase enzymatic activity in vitro, converting glyoxal (GO) or methylglyoxal (MGO) to glycolic or lactate, respectively [25–27]. Later, the apparent glyoxalase activity was recognized as deglycase activity, specifically catalyzing the deglycation of Maillard adducts formed between the amino groups of proteins or nucleotides and reactive carbonyl groups of glyoxal [28, 29]. Thus, cells with DJ-1 depletion exhibit increased levels of glycated DNA, DNA-strand breaks, and phosphorylated p53, providing another layer of intricacy to understand the promoting effect of DJ-1 knockdown on the efficacy of chemotherapeutic drugs in some tumor cells [30]. Hence, the deglycation activity of DJ-1 might indicate a new valuable direction for studying DJ-1 functions related to its cytoprotective effects, and the compounds inhibiting the deglycation activity of DJ-1 might serve as new tools to facilitate cancer therapy [11, 31].

Based on the publicly available protein structure database (PDB: 1PDV and 1PE0), the crystal structure of DJ-1 is a dimer comprising 11 β-sheets (β1-β11 sheets) and 8 α-helices (αA-αH helices) (Supplementary Fig. S1a, b) [32–34]. The helix–sheet–helix motif manifests a sandwiched structure [33]. The β3/β4 hairpin forms four antiparallel stretches, and the V51 residue located in the β4-sheet is crucial to this specific structure in dimeric DJ-1. The αA-helix motif is located in the center of the dimer structure, while the αH-helix motif in the C terminus of DJ-1 interacts with the β11′/αG′ loop of the co-monomer of the DJ-1 dimer [32–34]. It has been reported that the C-terminal G-helix–kink–H-helix motif is essential for protein stability and survival-promoting activity of the DJ-1 protein [35]. The L166P point mutant in the G-helix motif of DJ-1 is one of the most striking mutations to impair dimer formation, and it dramatically accelerates DJ-1 degradation [36–38]. Although more attention has been given to the C-terminal G-helix–kink–H-helix motif of DJ-1, the αG-helix motif has recently been recognized, while the function of the αH-helix motif has not been fully elucidated and remains characterized by theoretical prediction.

The aim of this study was to specifically investigate the influence of the C terminus on dimeric DJ-1 and its role in deglycation activity and ferroptosis. Through deletion mutations and point mutations, we deduced the most critical motif in the C terminus by attrition and found that the final three amino acids of the C terminus of DJ-1 (DJ-1 ΔC3), and notably, we found that its hydrophobic L187 residue is crucial for dimer formation and biological functions, specifically regulating DJ-1 homodimerization, deglycation activity and suppression of ferroptosis. The results of this study provide important insight that will fuel the future development of DJ-1 inhibitors targeting homodimerization as promising therapeutics for cancer therapy.

MATERIALS AND METHODS

Antibodies and reagents

The antibody to DJ-1 (#5933) was obtained from Cell Signaling Technology (Boston, America). The primary antibodies against GAPDH (db106), Myc (db2603) and Flag (db7002) were obtained from Diagnostic Biosystems (Hangzhou, China). MGO (W296902), GSH (G4251), and NAC (A7250) were obtained from Sigma-Aldrich (St. Louis, USA). Erastin (S7242) and ferrostatin-1 (S7243) were obtained from Selleck Chemicals (Houston, USA). DMEM (GIBCO, #12800) was obtained from Thermo Fisher Scientific (Waltham, MA, USA).

Cell culture

The HEK293T cell line was purchased from the Shanghai Institute of Biochemistry and Cell Biology (Shanghai, China). DJ-$1^{-/-}$ mouse embryonic fibroblast cells (MEFs) were produced from day 13.5 embryos of DJ-$1^{-/-}$ mice (B6.Cg-Park7tm1Shn, #006577, The Jackson Laboratory) according to standard procedures. The HEK293T and DJ-$1^{-/-}$ MEF cells were cultured in DMEM. All media were supplemented with 10% fetal bovine serum (HyClone, SV30160.03, GE Healthcare). The cells were incubated at 37 °C in a humidified atmosphere of 5% CO_2 and monitored for mycoplasma contamination every 6 months. HEK293T cells were authenticated by STR profiling.

DJ-1 expression and purification

The cDNA of DJ-1 and their mutants were cloned into pET28a vectors, which express N-terminal 6×His-tagged DJ-1 (the primers are listed in Supplementary Table S1). The cloned vectors were transformed into *E.coli* Trans BL21(DE3) (CD601-02, TransGen Biotech), which were grown at 37 °C in LB broth containing 0.1 mg/mL kanamycin until the OD_{600} reached 0.4–0.6. Isopropyl-β-*D*-thiogalactoside (IPTG, 0.25 mM) (V900917, Sigma-Aldrich) was then added, and bacteria were further incubated at 25 °C for 16 h. After centrifugation, the bacteria were resuspended in lysis buffer (20 mM Na_3PO_4, 500 mM NaCl, 50 mM imidazole, pH 7.4), homogenized by a high-pressure cell cracker and centrifuged (8000 × *g*) at 4 °C for 30 min. The supernatant was loaded onto the Ni^{2+}-NTA column, and the protein was eluted with 500 mM imidazole. The purified proteins were dialyzed with 100 mM Na_3PO_4 (pH 8.0) buffer containing 20% glycerinum.

Lentivirus titration assay

The lentivirus titration of all viruses was assayed using the qPCR lentivirus titration kit (#LV900, Applied Biological Materials) according to the manufacturer's instructions. Briefly, 2 μL of the virus was incubated with 18 μL of viral lysis buffer (#LV900-1) at room temperature for 3 min. Quantitative real-time RT-PCR analysis of the viral lysate was performed by iTaq^{TM} Universal SYBR Green Super Mix (#172–5124, Bio-Rad). The reaction mixtures containing SYBR Green were composed based on the manufacturer's protocol, and then, the CT values were obtained using a qPCR platform (QuantStudio 6 Flex Real-Time PCR System, Thermo Fisher Scientific). The titer was calculated according to the following formula: Titer of viral lysate $= 10 \times 5 \times 10^7/2^{3(Ctx\text{-}Ct1)/(Ct\text{x}\text{-}Ct2)}$. Ct_x = Ct values of the sample; Ct_1 = Ct values of lentivirus standard 1 (#LV900-3); Ct_2 = Ct values of lentivirus standard 2 (#LV900-4) (Supplementary Table S2).

Lentivirus transduction

The pCDH-EF1-Puro plasmid was obtained from System Biosciences. pCDH-DJ-1 WT and mutants were constructed using the primers listed in Supplementary Table S3. Lentivirus was generated by HEK293T cells with pCMV-dR8.91 (packaging vector), pMD2-VSVG (envelope vector), and targeted plasmids cotransfected using Lipofectamine 2000 (#11668019, Invitrogen). Medium containing virus was harvested 48 h after transfection and filtered through a 0.45-μm Millipore filter. Cells were grown in six-well plates to 20% to 30% confluency, and 0.1–1 mL of each virus was added with 2 μL of polybrene (6 mg/mL) (Supplementary Table S2). After the cells were infected for 16 h, the medium was exchanged for fresh medium.

Western blot analysis

Cells were lysed with 1% NP40 buffer (50 mM Tris-HCl;150 mM NaCl;1% NP40, pH 7.4;0.1 mM sodium vanadate; 5 μg/mL leupeptin; and 0.1 mM phenyl methane sulfonyl fluoride) and incubated at 4 °C for 30 min, flicked every 10 min to ensure cells were fully lysed. The lysate was then centrifuged at 12,000 × *g* for 30 min at 4 °C to remove insoluble materials. Protein concentrations of whole-cell lysates were determined with a QuantiProBCA assay kit (Sigma-Aldrich, QPBCA). The proteins were then electrophoresed in SDS-PAGE gels to separate them by molecular weight and transferred to polyvinylidene difluoride membranes (Millipore, Bedford, MA, USA). After blocking with 5% nonfat milk, the membrane was incubated overnight with the appropriate primary

antibody at 4 °C, followed by HRP-labeled secondary antibodies. Proteins were visualized using enhanced chemiluminescence detection (NEL103E001EA, PerkinElmer) with an AI600 imager (GE Healthcare).

Immunoprecipitation

Exogenous immunoprecipitation was performed with anti-Flag IP resin (L00425, GenScript) or anti-Myc magnetic beads (B26201, Bimake). Briefly, after the proteins were determined by the QuantiProBCA assay kit (QPBCA, Sigma-Aldrich), 500 μL of whole-cell lysates was added to a solution of magnetic beads for 8 h at 4 °C with end-over-end mixing. Finally, the complex was washed with T-PBS five times, suspended in 2× loading buffer and subjected to Western blot analysis.

DSS-mediated cross-linking assay

Whole-cell lysates were combined and incubated at 4 °C for 60 min in 2 mM disuccinimidyl suberate (DSS) cross-linker (suberic acid *bis* (*N*-hydroxysuccinimide ester), #S1885, Sigma), using isometric DMSO as a control. The reaction was quenched with 1 M Tris-HCl buffer (pH 7.4) for 15 min at room temperature. Samples were analyzed by Western blotting.

Size-exclusion chromatography (SEC)

One hundred microliters of purified recombinant protein (~2 mg/mL) were loaded onto a SEC column (PL1580-3301, Agilent) in phosphate buffer (20 mM Tris, 150 mM NaCl, pH 7.4) at run at 0.35 mL/min through a high-performance liquid chromatography column (1260 Infinity II, Agilent).

Glyoxalase assay

The purified wild-type DJ-1 protein or its mutants (6 μM) were mixed with MGO (final concentration 1.5 mM) in 50 mM sodium phosphate buffer (pH 7.0) at a total reaction volume of 70 μL at room temperature. The reaction was stopped by adding 120 μL of 0.1% 2,4-dinitrophenylhydrazine solution. The solution was incubated for 15 min at room temperature. Then, 160 μL of 10% NaOH was added. After further incubation for 15 min, the absorbance (540 nm for MGO) was measured.

Deglycase assay

Experiments were performed in 50 mM sodium phosphate buffer (pH 7.0) at room temperature. MGO and *N*-acetylcysteine were premixed to a final concentration of 2 mM. After reaching steady-state absorption levels at 288 nm, recombinant DJ-1 was added to a final concentration of 2 μM. An identical volume of sodium phosphate buffer was added as a control. The absorbance at 288 nm for hemi-thioacetal was measured for 60 min.

Analysis of lipid ROS production

Cells were harvested by trypsinization, resuspended in 500 μL of PBS containing 2 μM C11-BODIPY (581/591) (#D3861, Invitrogen) and incubated for 30 min at 37 °C in an incubator. The cells were then resuspended in 500 μL of fresh PBS, filtered through a 40-μm cell strainer, and analyzed using a flow cytometer (FACSuite, BD Biosciences) equipped with a 488-nm laser for excitation. The data were collected from the FL1 channel (527 nm). For each sample, at least 10,000 cells were analyzed.

Cell viability assay

Cell viability was assessed following typical procedures using a 96-well format and a Cell Counting Kit-8 (CCK-8) (HY-K0301, MedChemExpress). When added to cells, WST-8 [2-(2-methoxy-4-nitrophenyl)-3-(4-nitrophenyl)-5-(2,4-disulfophenyl)] is modified by the reductant produced by viable cells and turns orange (WST-8 formazan). Briefly, 10 μL of CCK-8 solution was added to each well of the plate and incubated for 1–4 h at 37 °C, and the absorbance was measured at 450 nm on a microplate reader (Multiskan spectrum 1500, Thermo). Cell viability for the test conditions was reported as a percentage relative to the negative control.

GSH assay

The relative GSH concentration in the cell lysates was assessed by a kit from Nanjing Jiancheng (#A006-2) following the manufacturer's instructions. The principle of this measurement is based on GSH reacting with dithiobisnitrobenzoic acid (DTNB). The yellow product (5-thio-2-nitrobenzoic acid) was measured spectrophotometrically at 405 nm. The values were normalized by protein concentration. The results are presented as fold changes relative to the negative control.

Statistical analysis

All statistical analyses were performed using Prism 7.0c (GraphPad Software). The number of biological replicates for each experiment is indicated in the figure legends. Values are presented as the means ± standard deviation (SD). Differences between means were determined using two-tailed, unpaired Student's *t* tests and were considered significant at $P < 0.05$.

RESULTS

The C terminus determines DJ-1-dimer formation

To investigate the dimerization of DJ-1, we first established stable DJ-1-overexpressing HEK293T cells using Flag-tagged and Myc-tagged DJ-1 lentivirus, with all tags located on the N-terminus; although some artificial effects of the tags were observed (Fig. 1a). Ectopic DJ-1 was purified from cells by immunoprecipitation. Our data illustrated that Myc-tagged DJ-1 was pulled down by Flag-tagged DJ-1 (Fig. 1b), and Flag-tagged DJ-1 was pulled down by Myc-tagged DJ-1 (Fig. 1c), indicating that DJ-1 had dimerized. Then, we studied the dimerization of DJ-1 by DSS, an intramolecular cross-linking agent that can prevent polymerized proteins avoid from disassembly in reductants, such as β-mercaptoethanol, during Western blot analysis. When the cell lysate was treated with DSS for 60 min at 4 °C, we found that the protein pulled down by both Flag-tagged and Myc-tagged DJ-1 represented a dimer (Fig. 1d). In addition, dimerization was also detected in the Flag-tagged and Myc-tagged DJ-1 coexpression system, suggesting that the N-terminus tag did not affect DJ-1 dimer formation (Fig. 1d).

It has been reported that the C-terminal G-helix–kink–H-helix motif is essential for the protein stability and survival-promoting activity of DJ-1 [35]. We explored how the C-terminal region affected the dimerization of DJ-1. Different deletion mutations, including DJ-1 ΔC6, ΔC15, ΔC17, ΔC23, and ΔC29, in its C terminus, were established with respect to the G-helix–kink–H-helix motif (Fig. 1e). The dimerization of the DJ-1 ΔC29 mutant was completely disrupted, a finding consistent with a previous report [35]. More interestingly, the DSS-mediated cross-linking assays showed the same results for the DJ-1 ΔC29 mutant when we narrowed the deletion region to the ΔC23, ΔC17, ΔC15 and, even to the ΔC6 mutants, indicating that the final six amino acids of the C terminus are important to DJ-1 dimerization (Fig. 1f). Next, we established successive deletion mutations in the last six amino acids, namely, DJ-1 ΔC1-ΔC6 (Fig. 1g), and when more than two amino acids were deleted, the dimerization of DJ-1 was remarkably affected, as indicated by the lack of DJ-1 ΔC3 dimer formation. When deleting the two amino acids K188 and D189, DJ-1 dimerization was partially affected, while deleting the D189 residue had no impact (Fig. 1h).

To further investigate whether this dimerization effect is influenced by size-dependent or localization-dependent amino acids, we reintroduced the mutants with three internal amino acids deleted from the C terminus: DJ-1 ΔC1-3(ΔC3), ΔC2-4, ΔC3-5, and ΔC4-6 (as illustrated in Fig. 1i). We then performed a DSS-

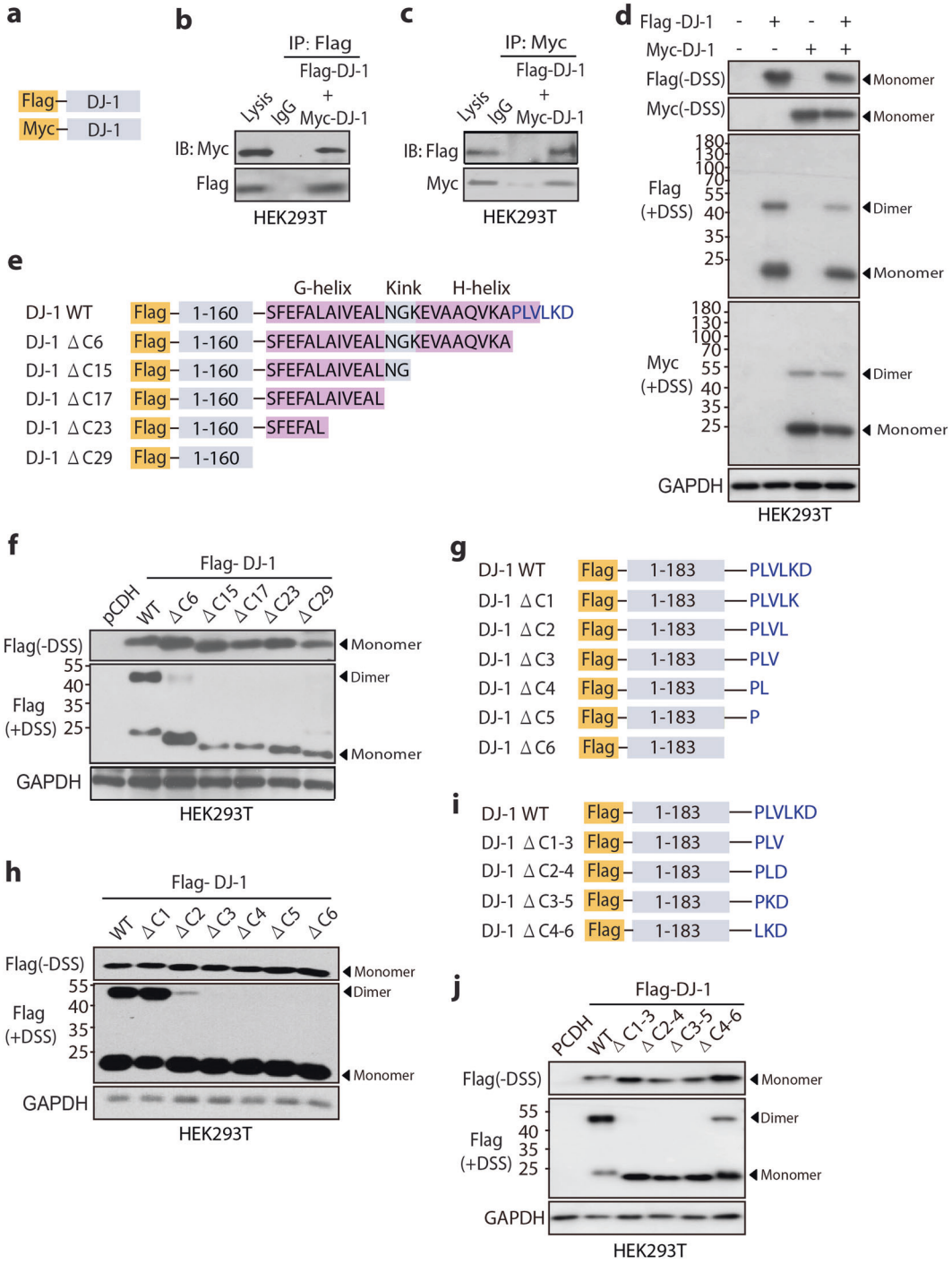

Fig. 1 The C terminus determines DJ-1 dimer formation. a Schematic of N-terminal tagged DJ-1. **b**, **c** The interaction between Flag-tagged and Myc-tagged DJ-1 was analyzed to indicate the extent of dimerization of the DJ-1 protein. The indicated HEK293T cells stably expressing Flag-tagged and Myc-tagged DJ-1 were harvested for immunoprecipitation and subjected to immunoblotting with anti-Flag antibodies (**b**) and anti-Myc antibodies (**c**). **d** Disuccinimidyl suberate (DSS) cross-linking assays of DJ-1 in the HEK293T cells with Flag-tagged and Myc-tagged DJ-1 overexpressed. **e** Schematic of deletion mutations in the C terminus of DJ-1, from DJ-1 ΔC29 to DJ-1 ΔC6. **f** DSS cross-linking assays of WT DJ-1 and mutants with deletions in the C terminus (ΔC29, ΔC23, ΔC17, ΔC15, and ΔC6) in the HEK293T cells. **g** Schematic of the deletion mutations in the C terminus of DJ-1, from DJ-1 ΔC6 to DJ-1 ΔC1. **h** DSS cross-linking assays of WT DJ-1 and mutants with deletions in the C terminus (ΔC6, ΔC5, ΔC4, ΔC3, ΔC2, and ΔC1) in the HEK293T cells. **i** Schematic of internal deletion mutations of three amino acids in the C terminus of DJ-1. **j** DSS cross-linking assays of WT DJ-1 and mutants with three internal amino acids deleted in the C terminus of DJ-1 in the HEK293T cells.

mediated cross-linking assay. The results showed that only the ΔC4-6 mutant retained DJ-1 dimerization capability, while ΔC2-4 and ΔC3-5 showed the same results as ΔC1-3, and in all of these mutants, the L187 amino acid was deleted (Fig. 1j). These results indicated a more localization-dependent than a size-dependent effect. Taken together, our data suggest that the last three amino acids in the C terminus, especially residues L187 and K188, play important roles in dimeric DJ-1 formation.

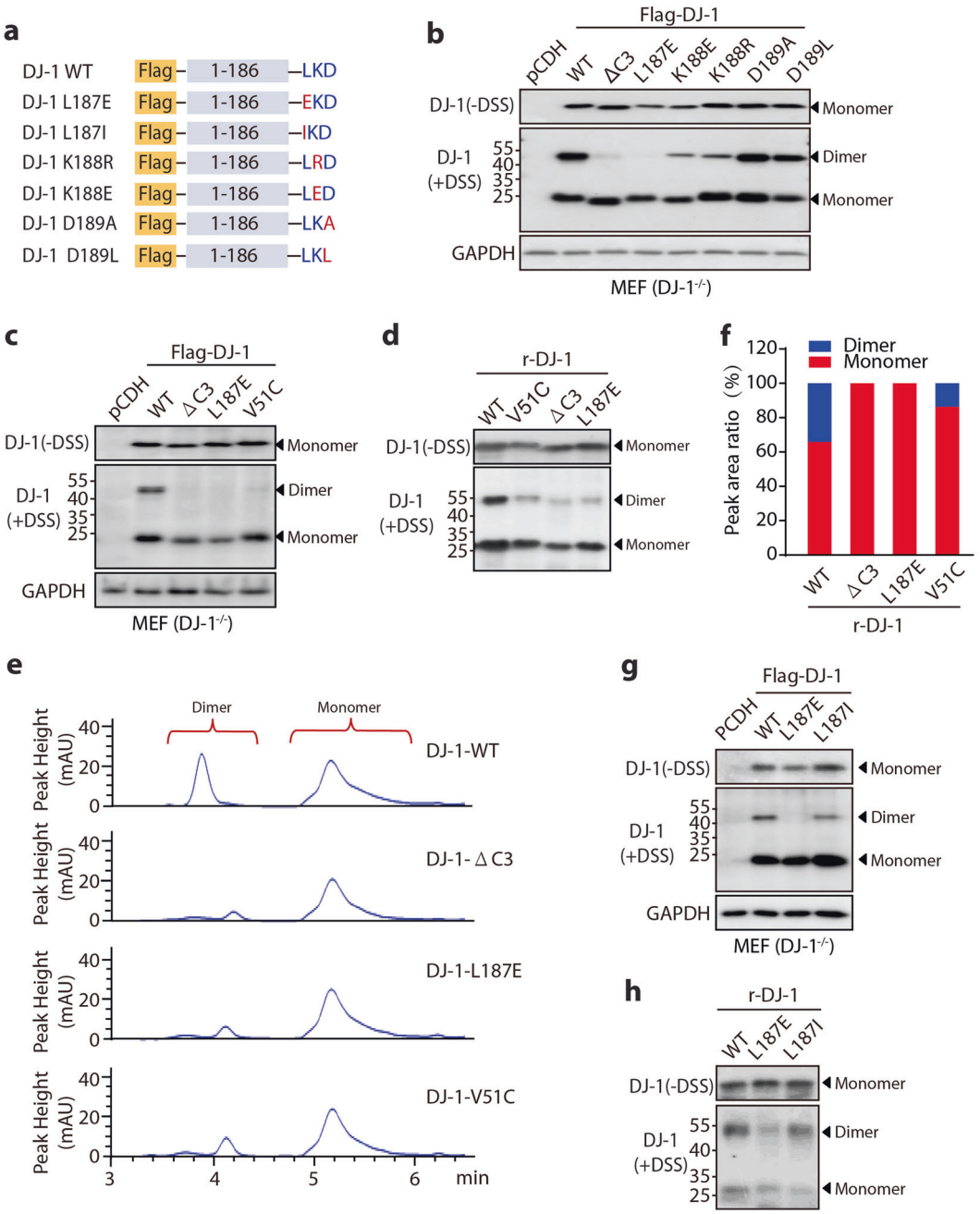

Fig. 2 The hydrophobic L187 residue is critical for DJ-1 homodimerization. a Schematic of point mutants in the C terminus of DJ-1. **b** Disuccinimidyl suberate (DSS) cross-linking assays of WT DJ-1 and point mutants in the C terminus in DJ-1$^{-/-}$ mouse embryonic fibroblasts (MEFs) with reintroduced DJ-1 proteins. **c** DSS cross-linking assays of WT DJ-1 and mutants (DJ-1 ΔC3, L187E, and V51C) in DJ-1$^{-/-}$ MEFs with reintroduced DJ-1 proteins. **d** DSS cross-linking assays of purified WT DJ-1 and mutant (DJ-1 ΔC3, L187E, and V51C) proteins. **e** Size-exclusion chromatography (SEC) analysis of purified WT DJ-1 and mutant (DJ-1 ΔC3, L187E, and V51C) proteins. **f** Quantitative analysis of (**e**). **g** DSS cross-linking assays of WT DJ-1 and mutants with point mutations (DJ-1 L187E and L187I) in the C terminus in DJ-1$^{-/-}$ MEFs with reintroduced DJ-1 proteins. **h** DSS cross-linking assays of purified WT DJ-1 and mutant (DJ-1 L187E and L187I) proteins.

The hydrophobic L187 residue is critical to DJ-1 homodimerization

The C terminus of DJ-1 consists of many hydrophobic and electrically charged amino acids, which may be critical for the homodimerization of DJ-1. To further study which residue among the last three amino acids at the C terminus plays the most important role in dimeric DJ-1 formation, we established various point mutants based on the three residues according to their charge and hydrophobic properties (Fig. 2a). Given that the endogenous DJ-1 protein might have effects on the homodimerization of ectopic DJ-1, we utilized embryonic DJ-1$^{-/-}$ mouse fibroblast cells (DJ-1$^{-/-}$ MEFs) to exclude interference by endogenous DJ-1. When we reintroduced human WT DJ-1 and its mutants with point mutations into DJ-1$^{-/-}$ MEFs, we found that the D189A and D189L mutants had little impact on DJ-1 homodimerization, as their dimeric DJ-1 level was similar to that of wild-type DJ-1 (Fig. 2b). The homodimerization of K188E and K188R DJ-1 mutants was partially decreased according to the DSS-mediated cross-linking assay (Fig. 2b). Interestingly, when we reintroduced the L187E mutant

into DJ-1$^{-/-}$ MEFs, dimeric DJ-1 completely disappeared, which was the same outcome as exhibited by DJ-1 ΔC3 (Fig. 2b). The V51 residue located at the β4-sheet is important for homodimerization based on the crystal structure, because it serves as a bridge between two DJ-1 monomers at a different surface C terminus of DJ-1 [12, 33–35]. Then, we reintroduced the V51C mutant as a control to further study the importance of the C terminus to DJ-1. When the DJ-1 ΔC3 and L187E mutants were reintroduced along with WT and V51C mutant DJ-1 into the DJ-1$^{-/-}$ MEFs, we found that the V51C mutant interfered completely with homodimerization of DJ-1, as expected (Fig. 2c). The DJ-1 ΔC3 and L187E mutants also absolutely suppressed dimeric DJ-1 formation, similar to the V51C mutant (Fig. 2c).

After investigating the influence of the C terminus on DJ-1 homodimerization at the cellular level, we asked whether purified proteins would lead to the same phenomenon. We cloned wild-type DJ-1 and its ΔC3, L187E, and V51C mutants into pET28a vectors, which express N-terminal 6×His-tagged. Then, the cloned vectors were transformed into *E. coli* BL21(DE3) to express different DJ-1 proteins. The expressed DJ-1 proteins were purified on a Ni^{2+}-NTA column, and the eluent was detected by SDS-PAGE (Supplementary Fig. S2a–d). The eluent containing DJ-1 proteins was then subjected to dialysis in phosphate-buffered saline, and the purity was determined. The Coomassie brilliant blue staining results showed that the proteins were purified adequately (Supplementary Fig. S1f). Next, we utilized the purified proteins to perform a DSS-mediated cross-linking assay, and the results indicated that three mutants of DJ-1 significantly inhibited dimeric formation compared to the effect of WT DJ-1 (Fig. 2d). In addition, the results of SEC showed that ~33% of the protein was a dimer in the WT DJ-1 protein, while the ratio of the DJ-1 V51C mutant was nearly 15%, and there were few DJ-1 dimers detected among the DJ-1 ΔC3 and L187E mutants when the smallest detected peak area was set to 50 mAU*s (Fig. 2e, f).

To validate the importance of the hydrophobicity of the L187 residue, the L187I mutant, with a similar hydrophobic amino acid, was introduced. The recombinant L187I mutant with an N-terminal 6×His-tag was purified and subjected to dialysis similar to the other recombinant proteins (Supplementary Fig. S2e, f). DSS-mediated cross-linking assays indicated that the DJ-1 L187I mutant still formed a high proportion of dimers both in the DJ-1$^{-/-}$ MEFs and in vitro compared with the L187E mutant (Fig. 2g, h). These results confirmed that the C terminus of DJ-1, especially the hydrophobic L187 residue, is critical to the homodimerization of DJ-1.

The C terminus of DJ-1 affects its MGO detoxification activity

MGO produced by glucose oxidation, lipid peroxidation and DNA oxidation is a reactive metabolite that forms adducts on the cysteine, lysine, and arginine residues of a protein [39]. MGO is converted into D-lactate by two enzymes, glyoxalase 1 (Glo 1) and glyoxalase 2 (Glo 2), in the glyoxalase system via a mechanism requiring reduced GSH [40]. DJ-1 has been characterized as another glyoxalase in vitro, directly converting MGO into lactate without GSH (Fig. 3a). The Richarm group suggested that this glyoxalase activity is truly deglycase activity, through which MGO adducts are enzymatically removed from protein side chains, such as those on cysteine (Fig. 3b) [31]. The glyoxalase and deglycase activity can be summarized as the MGO detoxification ability of DJ-1 [39]. What we next wanted to investigate was whether the C terminus of DJ-1 has effects on the MGO detoxification ability of DJ-1. First, we performed a glyoxalase assay utilizing purified protein, and the results showed that the consumption of MGO was enormously different between wild-type DJ-1 and its mutant counterparts. MGO consumption was significantly decreased in the purified DJ-1 mutants compared with the purified wild-type DJ-1, suggesting that glyoxalase activity was inhibited dramatically by both DJ-1 ΔC3 and L187E mutants, and the suppression effect was the same as that of the V51C mutant (Fig. 3c). Then, we investigated the deglycase activity of the DJ-1 ΔC3 and L187E mutants. The absorbance at 288 nm revealed the level of hemi-thioacetal, the intermediate in the reaction of MGO and *N*-acetylcysteine, which could be ultimately converted into lactate by DJ-1. The results showed that the decrease in hemi-thioacetal was obviously inhibited in the DJ-1 ΔC3, L187E, and V51C mutants, indicating that the deglycase activity of these mutants was suppressed (Fig. 3d). These data implied that the MGO detoxification ability of DJ-1 was regulated by its C terminus, specifically the hydrophobic L187 residue, in vitro.

Next, we studied the influence of the DJ-1 C terminus on the MGO detoxification ability in cells. In addition to overexpressed DJ-1 protein, Glo 1 and Glo 2 in the glyoxalase system also convert MGO into lactate [40]. MGO-glycated proteins containing cysteine, arginine, and lysine residues could only be repaired by DJ-1 through the action of different intermediate metabolites (Fig. 3e). We thus established stable overexpressed WT and a series of DJ-1 mutations in DJ-1$^{-/-}$ MEFs to test the influence of the DJ-1 C terminus on the MGO detoxification ability. After treatment with 2 mM MGO, the cells were centrifuged and lysed to determine the level of MGO-glycated proteins by a specific anti-MGO antibody. As expected, our results suggested that MGO was consumed distinctly by wild-type DJ-1, indicating that WT DJ-1 has MGO detoxification ability in cells (Fig. 3f). Notably, the MGO level was partially reversed in the DJ-1 ΔC3 mutant and absolutely reversed in the DJ-1 L187E mutant (Fig. 3f), suggesting that the C terminus of DJ-1 affects its MGO detoxification ability in cells.

The C terminus of DJ-1 regulates its suppression of ferroptosis

Given that a recent study suggested that DJ-1 could suppress ferroptosis triggered by lipid ROS, the impact of the DJ-1 C terminus on the suppression of ferroptosis was next investigated [19]. We utilized erastin, a classic ferroptosis inducer, to build a model of ferroptosis. Erastin is a nonspecific inhibitor of SLC7A11, decreasing the uptake of cystine and blocking glutathione synthesis and finally inducing the accumulation of membrane lipid ROS and ferroptosis [41, 42]. Moreover, to validate the effects of the DJ-1 C terminus on DJ-1 regulation of the ferroptosis process, ferrostatin-1(Fer-1), a specific inhibitor of ferroptosis, was used. Fer-1 is a lipid ROS scavenger with an N-cyclohexyl portion that acts as a lipid anchor within the biofilm. First, WT DJ-1 and three mutants, namely, DJ-1 ΔC3, L187E, and V51C, were reintroduced into DJ-1$^{-/-}$ MEFs (Fig. 4a). Then, after treatment with erastin and Fer-1 for 12 h, the cells were centrifuged before flow cytometry was performed using the C11-BODIPY, a fluorescent radioprobe for indexing lipid peroxidation, a classic biomarker of ferroptosis. The results showed that overexpression of wild-type DJ-1 significantly inhibited erastin-induced accumulation of lipid ROS, and the V51C mutant had partial inhibitory effects. The DJ-1 ΔC3 and L187E mutants had little effect on the accumulation of lipid ROS induced by erastin. Notably, Fer-1 treatment completely reversed erastin-induced lipid accumulation (Fig. 4b, c).

Moreover, the effect of DJ-1 on erastin-triggered ferroptotic cell death was also examined. As shown in Fig. 4d, e, wild-type DJ-1 played a significant inhibitory role in the effect of erastin-triggered ferroptotic cell death, and the suppression of ferroptosis was eliminated when the C terminus of DJ-1 was mutated as ΔC3 and L187E. The DJ-1 V51C mutant exhibited weak partial suppression of ferroptosis. In addition, erastin-induced cell death was completely reversed when combined with Fer-1, which was consistent with the lipid ROS level results (Fig. 4d, e). Furthermore, the GSH level was partially reversed under erastin treatment when and only when WT DJ-1 was overexpressed, which agreed with the results presented above (Fig. 4f). Therefore, our results further implied that the C terminus of DJ-1 mediates the suppression of

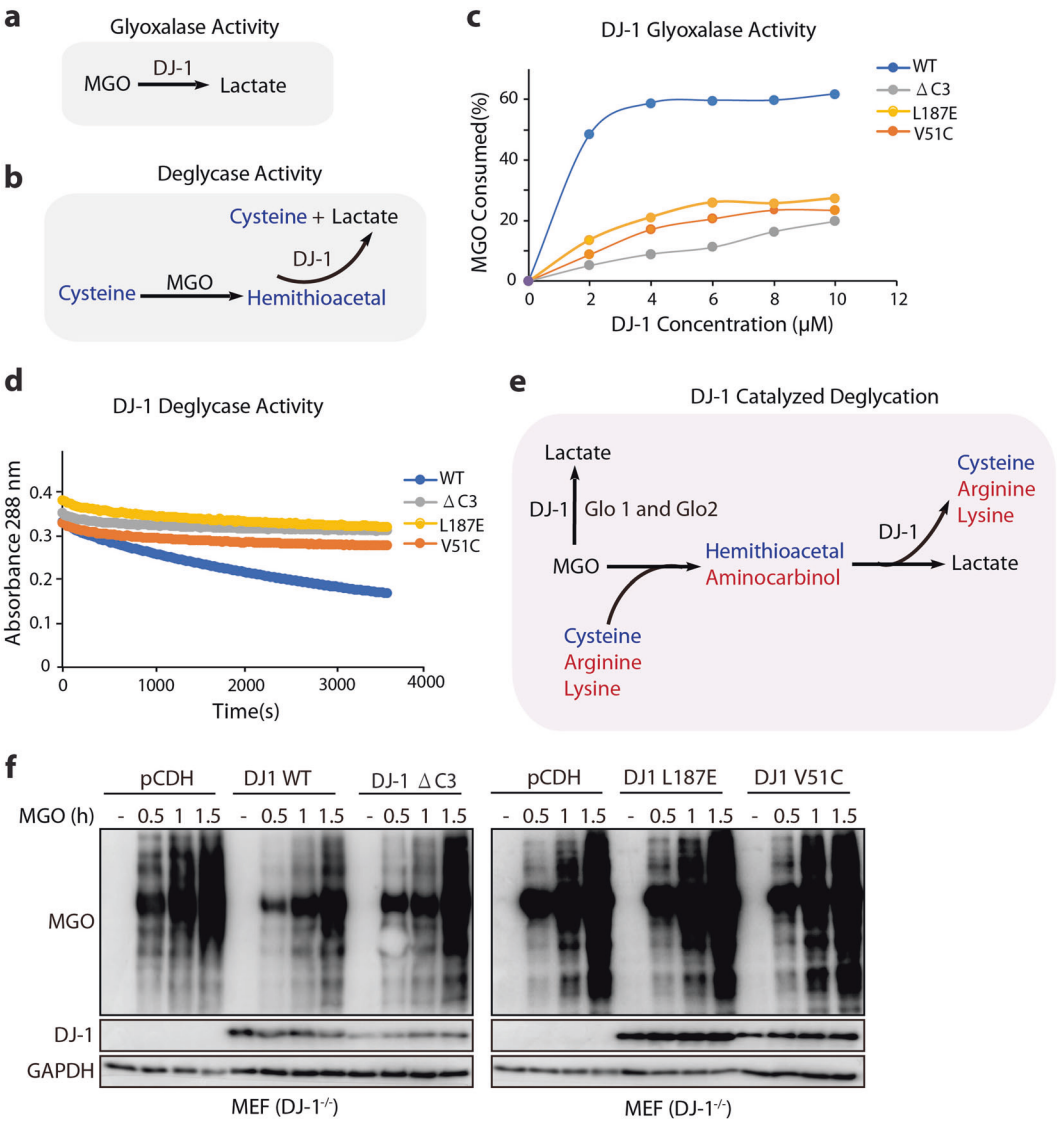

Fig. 3 The C terminus of DJ-1 affects its MGO detoxification activity. a, **b** Schematic of DJ-1 glyoxalase activity (**a**) and deglycase activity (**b**). **c** Glyoxalase assay of purified WT DJ-1 and mutants (DJ-1 ΔC3, L187E, and V51C), absorbance (540 nm for MGO) was measured. **d** Deglycase assay of purified WT DJ-1 and mutants (DJ-1 ΔC3, L187E, and V51C). Absorbance (288 nm for hemi-thioacetal) was measured for 60 min. **e** Schematic of DJ-1-catalyzed deglycation in DJ-$1^{-/-}$ mouse embryonic fibroblasts (MEFs) with reintroducing DJ-1 proteins. **f** DJ-$1^{-/-}$ MEFs with different reintroduced human DJ-1 proteins were treated with 2 mM MGO for 0.5, 1, and 1.5 h, the cells were harvested, and the expression of DJ-1 and MGO-glycated protein was analyzed by Western blot. The relative gene expression was normalized to that of GAPDH.

ferroptosis, and when the C-terminal structure is destroyed, DJ-1 inhibition of ferroptosis is abolished.

DISCUSSION

DJ-1 is a multifunctional protein associated with both neurodegeneration and neoplasia, and it is believed that DJ-1 carries out its function exclusively in the dimeric state [16, 43, 44]. In our previous study, dimeric DJ-1 depolymerized apoptosis was regulated by fenretinide (4-HPR), indicating that the homodimerization of DJ-1 may be critical to its function [20]. The pathogenic L166P mutant of DJ-1 is critical for PD because it impairs the neuronal cytoprotective function of DJ-1 by interfering with dimer formation and protein stability [45]. It is interesting to investigate whether the mutation-induced loss of function causes the disappearance of homodimerization or whether it impacts DJ-1 protein stability. Our studies showed that the monomeric DJ-1 ΔC3 and L187E mutants were stable because no significant protein degradation was observed compared with the WT DJ-1 degradation both in cells and in vitro, an outcome that differs from that of the L166P mutant. These results indicated that the level of homodimerization may not fully represent the stability of the DJ-1 protein and that the DJ-1 mutants ΔC3 and L187E may be the most useful tools for studying the function of dimeric DJ-1.

It has been reported that the G-helix and kink motif are important because they determine the C-terminal helix–kink–helix, which is essential for the protein stability and survival-promoting activity of DJ-1 [35]. In addition, the pathogenic L166P mutant induces a loss of DJ-1 function, and instead of forming a dimeric structure, it assembles into high molecular weight oligomers [45, 46]. In terms of the structure of DJ-1, L166 is located in the middle of the G-helix motif, and its mutation breaks the helix [45]. The hydrophobic interactions with a series of residues located at the subunit–subunit interface, including V181, K182, and L187 of the C terminus, may affect the stability of the homodimer [47]. However, this hypothesis has yet to be proven by

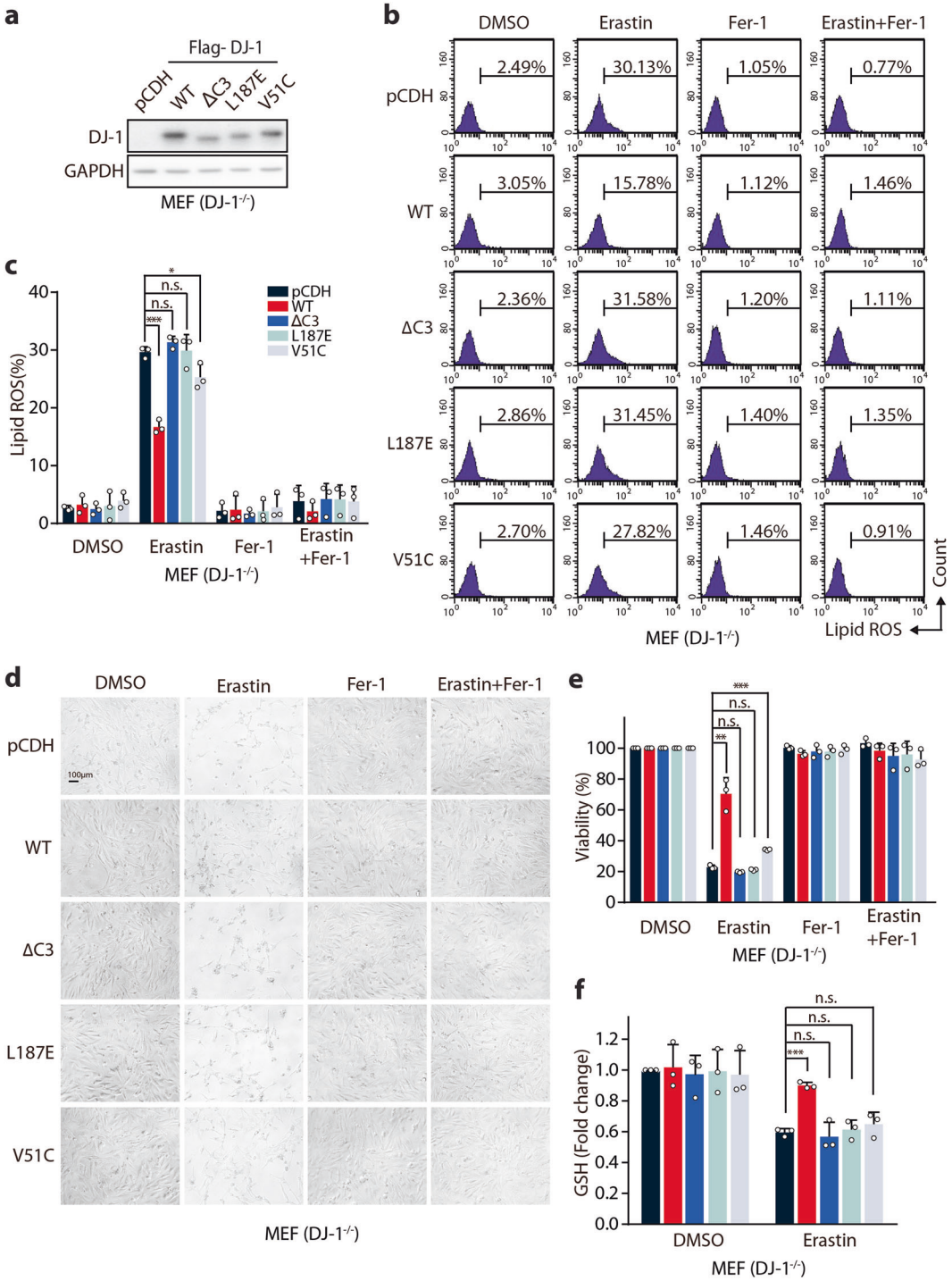

Fig. 4 The C terminus of DJ-1 regulates its suppression of ferroptosis. a Western blot analysis of DJ-1 expression in DJ-$1^{-/-}$ mouse embryonic fibroblasts (MEFs) with reintroduced human WT DJ-1 and mutant proteins. **b** The indicated MEFs were treated with erastin (400 nM) with or without ferrostatin-1 (Fer-1, 400 nM) for 12 h, and lipid ROS production was assayed by flow cytometry using C11-BODIPY. Representative data are shown. **c** Quantitative analysis of (**b**). The statistical analysis is based on three independent experiments. **d** Phase-contrast images of the indicated MEFs treated with 400 nM erastin with or without Fer-1 (400 nM) for 24 h. Independent experiments were repeated three times. Representative data are shown. **e** The indicated MEFs treated with 400 nM erastin with or without Fer-1 (400 nM) for 24 h were tested for viability. **f** The indicated MEFs were treated with erastin (400 nM) for 6 h, and then, the relative GSH level was assayed. The statistical analysis was performed with the results from three independent experiments. All the data are representative of three independent experiments, and the error bar indicates the s.d. value. $^{*}P < 0.05$; $^{**}P < 0.01$; $^{***}P < 0.001$.

analysis of conformational changes or experiments in vitro. In this study, with MEF (DJ-$1^{-/-}$) cells and recombinant proteins, we confirmed that wild-type DJ-1 undergoes homodimerization and that the C terminus is crucial for the stability of dimeric DJ-1 proteins. The critical motif in the C terminus determined by elimination to be the final three amino acids, and further research showed that the hydrophobic L187 residue played the most important role in DJ-1 homodimerization. These data supported

the hypothesis that hydrophobic interactions may affect the stability of the DJ-1 homodimer, prompting studies on other hydrophobic residues located at the subunit–subunit interface. Moreover, multiple charged amino acids in the C terminus provide a better site for compound intervention than the flat β3-β4 hairpin structure. Probes designed based on the hydrophobic C terminus of DJ-1 are useful tools for carrying out research on DJ-1 structure and function. The inhibitors of dimeric DJ-1, which may have synergistic antitumor effects, can be designed according to the structure of the hydrophobic C terminus.

According to the experiments on the function of DJ-1, the C terminus was critical for MGO detoxification and suppression of ferroptosis. The glyoxalase and deglycase activities of DJ-1 repair MGO- and GO-glycated nucleotides and proteins, showing that DJ-1 plays a cytoprotective role [30, 31, 40]. We found that the hydrophobic C terminus, especially the L187 residue, was crucial for DJ-1 MGO detoxification because both deglycase and glyoxalase activities were completely inhibited by the L187E mutant in vitro. The effects in the cells did not completely align with the results obtained in vitro, as DJ-1 ΔC3 had residual effects on MGO detoxification activity. We think that this outcome was probably complicated by the multiple functions of DJ-1 in cells. In addition, Glo 1 and Glo 2 participated in MGO detoxification, and the levels of Glo 1 and Glo 2 also impacted the MGO level. Given the crucial influence of the C terminus on MGO detoxification, in vitro deglycase activity and glyoxalase activity assays can be effectively used to screen inhibitors of dimeric DJ-1.

In addition, the suppression of ferroptosis was consistent with MGO detoxification ability, as DJ-1 ΔC3 and L187E mutants lost the ability to inhibit ferroptosis compared with the ability of WT DJ-1. In addition, the suppression was more obvious for the DJ-1 ΔC3 and L187E mutants than for the V51C mutant, indicating that the hydrophobic C terminus may have other effects, such as regulation of signaling pathways [5, 7, 48]. All these data supported our previous discovery that DJ-1 is a negative modulator of ferroptosis, providing new opportunities to facilitate ferroptosis-based cancer therapy [19]. We also examined the expression of glutathione peroxidase 4 (GPX4), a key molecule involved in ferroptosis. The results showed that the expression of GPX4 was not affected in cells overexpressing various DJ-1 mutants after treatment with erastin (Supplementary Fig. S3). This result was probably because erastin did not directly inhibit GPX4, but affected SLC7A11, decreasing the uptake of cystine and blocking glutathione synthesis. Therefore, the effects of erastin on ferroptosis may not be affected by GPX4 expression or activity and instead acts on its co-factor glutathione through the cystine/glutamate transporter SLC7A11. DJ-1 functioned on the upstream of GPX4, maintaining the level of cysteine synthesized from the transsulfuration pathway when SLC7A11 was inhibited, according to a previous report [19].

Taken together, the findings of this study showed that the hydrophobic C-terminal region of DJ-1 regulated DJ-1 homodimerization, MGO detoxification activity and suppression of ferroptosis. They are valuable supplements to the existing studies on the relationship between the structure and functions of DJ-1. They also provide useful ideas and directions for designing and screening inhibitors of DJ-1, which may have potential antitumor effects [49, 50].

ACKNOWLEDGEMENTS

This work was supported by grants from National Science & Technology Major Project "Key New Drug Creation and Manufacturing Program", China (2018ZX09711002 to HZ), the National Natural Science Foundation of China (No. 81773757 to MDY; No. 81402951 to JC), and Zhejiang Medical and Health Science and Technology Program (No. 2020384517 to CYD).

AUTHOR CONTRIBUTIONS

JC, LJ, and XBC designed the research and wrote the paper; LJ, XBC, QW, HYZ, CYD performed the biochemical and cellular studies; JC, LJ, XBC, HZ, and MDY analyzed the results; JC, HZ, MDY, QJH, and BY directed the study.

ADDITIONAL INFORMATION

The online version of this article (https://doi.org/10.1038/s41401-020-00531-1) contains supplementary material, which is available to authorized users.

Competing interests: The authors declare that they have no conflict of interest.

REFERENCES

1. Nagakubo D, Taira T, Kitaura H, Ikeda M, Tamai K, Iguchi-Ariga SMM, et al. DJ-1, a novel oncogene which transforms mouse NIH3T3 cells in cooperation with ras. Biochem Biophys Res Commun. 1997;231:509–13.
2. Zhang L, Shimoji M, Thomas B, Moore D, Yu S-W, Marupudi N, et al. Mitochondrial localization of the Parkinson's disease related protein DJ-1: implications for pathogenesis. Hum Mol Genet. 2005;14:2063–73.
3. Bonifati V, Rizzu P, Baren M, Schaap O, Breedveld G, Krieger E, et al. Mutations in the DJ-1 gene associated with autosomal recessive early-onset parkinsonism. Science. 2003;299:256–9.
4. Le Naour F, Misek DE, Krause MC, Deneux L, Giordano TJ, Scholl S, et al. Proteomics-based identification of RS/DJ-1 as a novel circulating tumor antigen in breast cancer. Clin Cancer Res. 2001;7:3328–35.
5. Oh SE, Mouradian MM. Cytoprotective mechanisms of DJ-1 against oxidative stress through modulating ERK1/2 and ASK1 signal transduction. Redox Biol. 2018;14:211–7.
6. Tian M, Cui YZ, Song GH, Zong MJ, Zhou XY, Chen Y, et al. Proteomic analysis identifies MMP-9, DJ-1 and A1BG as overexpressed proteins in pancreatic juice from pancreatic ductal adenocarcinoma patients. BMC Cancer. 2008;8:241.
7. Cao J, Lou S, Ying M, Yang B. DJ-1 as a human oncogene and potential therapeutic target. Biochem Pharmacol. 2014;93:241–50.
8. Kim RH, Peters M, Jang Y, Shi W, Pintilie M, Fletcher GC, et al. DJ-1, a novel regulator of the tumor suppressor PTEN. Cancer Cell. 2005;7:263–73.
9. Takahashi-Niki K, Kato-Ose I, Murata H, Maita H, Ariga S, Ariga H. Epidermal growth factor-dependent activation of the extracellular signal-regulated kinase pathway by DJ-1 protein through its direct binding to c-Raf protein. J Biol Chem. 2015;290:17838–47.
10. Clements C, McNally R, Conti B, Duncan G, Ting J. DJ1, a cancer and Parkinson's disease-associated protein, stabilizes the antioxidant transcriptional master regulator Nrf2. Proc Natl Acad Sci USA. 2006;103:15091–6.
11. Bahmed K, Boukhenouna S, Karim L, Andrews T, Lin J, Powers R, et al. The effect of cysteine oxidation on DJ-1 cytoprotective function in human alveolar type II cells. Cell Death Dis. 2019;10:638.
12. Kiss R, Zhu M, Jójárt B, Czajlik A, Solti K, Fórizs B, et al. Structural features of human DJ-1 in distinct Cys106 oxidative states and their relevance to its loss of function in disease. Biochim Biophys Acta Gen Subj. 2017;1861:2619–29.
13. Wilson MA. The role of cysteine oxidation in DJ-1 function and dysfunction. Antioxid Redox Signal. 2011;15:111–22.
14. Kinumi T, Kimata J, Taira T, Ariga H, Niki E. Cysteine-106 of DJ-1 is the most sensitive cysteine residue to hydrogen peroxide-mediated oxidation in vivo in human umbilical vein endothelial cells. Biochem Biophys Res Commun. 2004;317:722–8.
15. Taira T, Saito Y, Niki T, Iguchi-Ariga SMM, Takahashi K, Ariga H. DJ-1 has a role in antioxidative stress to prevent cell death. EMBO Rep. 2004;5:213–8.
16. Canet-Avilés RM, Wilson MA, Miller DW, Ahmad R, McLendon C, Bandyopadhyay S, et al. The Parkinson's disease protein DJ-1 is neuroprotective due to cysteine-sulfinic acid-driven mitochondrial localization. Proc Natl Acad Sci USA. 2004;101:9103–8.
17. Blackinton J, Lakshminarasimhan M, Thomas KJ, Ahmad R, Greggio E, Raza AS, et al. Formation of a stabilized cysteine sulfinic acid is critical for the mitochondrial function of the parkinsonism protein DJ-1. J Biol Chem. 2009;284:6476–85.
18. Raninga P, Di Trapani G, Tonissen K. The multifaceted roles of DJ-1 as an antioxidant. In: Ariga H, Iguchi-Ariga SMM, editors. DJ-1/PARK7 protein. Singapore: Springer; 2017. p. 67–87.
19. Cao J, Chen X, Jiang L, Lu B, Yuan M, Zhu D, et al. DJ-1 suppresses ferroptosis through preserving the activity of S-adenosyl homocysteine hydrolase. Nat Commun. 2020;11:1251.

20. Cao J, Ying M, Xie N, Lin G, Dong R, Zhang J, et al. The oxidation states of DJ-1 dictate the cell fate in response to oxidative stress triggered by 4-hpr: autophagy or apoptosis? Antioxid Redox Signal. 2014;21:1443–59.
21. Dolgacheva LP, Berezhnov AV, Fedotova EI, Zinchenko VP, Abramov AY. Role of DJ-1 in the mechanism of pathogenesis of Parkinson's disease. J Bioenerg Biomembr. 2019;51:175–88.
22. Xu C-Y, Kang W-Y, Chen Y-M, Jiang T-F, Jia Z, Zhang L-N, et al. DJ-1 inhibits α-synuclein aggregation by regulating chaperone-mediated autophagy. Front Aging Neurosci. 2017;9:308.
23. Meulener MC, Graves CL, Sampathu DM, Armstrong-Gold CE, Bonini NM, Giasson BI. DJ-1 is present in a large molecular complex in human brain tissue and interacts with α-synuclein. J Neurochem. 2005;93:1524–32.
24. Inden M, Taira T, Kitamura Y, Yanagida T, Tsuchiya D, Takata K, et al. PARK7 DJ-1 protects against degeneration of nigral dopaminergic neurons in Parkinson's disease rat model. Neurobiol Dis. 2006;24:144–58.
25. Lee J-y, Song J, Kwon K, Jang S, Kim C, Baek K, et al. Human DJ-1 and its homologs are novel glyoxalases. Hum Mol Genet. 2012;21:3215–25.
26. Subedi KP, Choi D, Kim I, Min B, Park C. Hsp31 of *Escherichia coli* K-12 is glyoxalase III. Mol Microbiol. 2011;81:926–36.
27. Misra K, Banerjee AB, Ray S, Ray M. Glyoxalase III from *Escherichia coli*: a single novel enzyme for the conversion of methylglyoxal into D-lactate without reduced glutathione. Biochem J. 1995;305:999–1003.
28. Richarme G, Marguet E, Forterre P, Ishino S, Ishino Y. DJ-1 family Maillard deglycases prevent acrylamide formation. Biochem Biophys Res Commun. 2016;478:1111–6.
29. Mihoub M, Abdallah J, Richarme G. Protein repair from glycation by glyoxals by the DJ-1 family Maillard deglycases. In: Ariga H, Iguchi-Ariga SMM, editors. DJ-1/PARK7 protein. Singapore: Springer; 2017. p. 133–47.
30. Richarme G, Liu C, Mihoub M, Abdallah J, Léger T, Joly N, et al. Guanine glycation repair by DJ-1/Park7 and its bacterial homologs. Science. 2017;357:208–11.
31. Richarme G, Mihoub M, Dairou J, Bui L-C, Léger T, Lamouri A. Parkinsonism-associated protein DJ-1/Park7 is a major protein deglycase that repairs methylglyoxal- and glyoxal-glycated cysteine, arginine, and lysine residues. J Biol Chem. 2015;290:1885–97.
32. Honbou K, Noda N, Horiuchi M, Niki T, Taira T, Ariga H, et al. The crystal structure of DJ-1, a protein related to male fertility and Parkinson's disease. J Biol Chem. 2003;278:31380–4.
33. Tao X, Tong L. Crystal structure of human DJ-1, a protein associated with early onset Parkinson's disease. J Biol Chem. 2003;278:31372–9.
34. Wilson MA, Collins JL, Hod Y, Ringe D, Petsko GA. The 1.1-Å resolution crystal structure of DJ-1, the protein mutated in autosomal recessive early onset Parkinson's disease. Proc Natl Acad Sci USA. 2003;100:9256–61.
35. Görner K, Holtorf E, Waak J, Pham T-T, Vogt Weisenhorn D, Wurst W, et al. Structural determinants of the C-terminal helix-kink-helix motif essential for protein stability and survival promoting activity of DJ-1. J Biol Chem. 2007;282:13680–91.
36. Alvarez-Castelao B, Muñoz C, Sánchez I, Goethals M, Vandekerckhove J, Castaño J. Reduced protein stability of human DJ-1/PARK7 L166P, linked to autosomal recessive Parkinson disease, is due to direct endoproteolytic cleavage by the proteasome. Biochim Biophys Acta. 2011;1823:524–33.
37. Anderson P, Daggett V. Molecular basis for the structural instability of human DJ-1 induced by the L166P mutation associated with Parkinson's disease †. Biochemistry. 2008;47:9380–93.
38. Miller D, Ahmad R, Hague S, Canet-Aviles R, McLendon C, Carter D, et al. L166P mutant DJ-1, causative for recessive Parkinson's disease, is degraded through the ubiquitin-proteasome system. J Biol Chem. 2003;278:36588–95.
39. Pfaff D, Fleming T, Nawroth P, Teleman A. Evidence against a role for the Parkinsonism-associated protein DJ-1 in methylglyoxal detoxification. J Biol Chem. 2016;292:685–90.
40. Thornalley P. Glyoxalase I—structure, function and a critical role in the enzymatic defence against glycation. Biochem Soc Trans. 2003;31:1343–8.
41. Zhou H-H, Chen X, Cai LY, Nan XW, Chen JH, Chen XX, et al. Erastin reverses ABCB1-mediated docetaxel resistance in ovarian cancer. Front Oncol. 2019;9:1398.
42. Xie Y, Hou W, Song X, Yu Y, Huang J, Sun X, et al. Ferroptosis: process and function. Cell Death Differ. 2016;23:369–79.
43. Chan J, Chan SHH. Activation of endogenous antioxidants as a common therapeutic strategy against cancer, neurodegeneration and cardiovascular diseases: a lesson learnt from DJ-1. Pharmacol Ther. 2015;156:69–74.
44. Moore DJ, Zhang L, Troncoso J, Lee MK, Hattori N, Mizuno Y, et al. Association of DJ-1 and parkin mediated by pathogenic DJ-1 mutations and oxidative stress. Hum Mol Genet. 2005;14:71–84.
45. Olzmann JA, Brown K, Wilkinson KD, Rees HD, Huai Q, Ke H, et al. Familial Parkinson's disease-associated L166P mutation disrupts DJ-1 protein folding and function. J Biol Chem. 2004;279:8506–15.
46. Baulac S, LaVoie MJ, Strahle J, Schlossmacher MG, Xia W. Dimerization of Parkinson's disease-causing DJ-1 and formation of high molecular weight complexes in human brain. Mol Cell Neurosci. 2004;27:236–46.
47. Herrera FE, Zucchelli S, Jezierska A, Lavina ZS, Gustincich S, Carloni P. On the oligomeric state of DJ-1 protein and its mutants associated with Parkinson disease. A combined computational and in vitro study. J Biol Chem. 2007;282:24905–14.
48. Fernandez-Caggiano M, Schröder E, Cho H-J, Burgoyne J, Barallobre-Barreiro J, Mayr M, et al. Oxidant-induced interprotein disulfide formation in cardiac protein DJ-1 occurs via an interaction with peroxiredoxin 2. J Biol Chem. 2016;291:10399–410.
49. Drechsel J, Mandl FA, Sieber SA. Chemical probe to monitor the parkinsonism-associated protein DJ-1 in live cells. ACS Chem Biol. 2018;13:2016–9.
50. Tashiro S, Caaveiro JMM, Nakakido M, Tanabe A, Nagatoishi S, Tamura Y, et al. Discovery and optimization of inhibitors of the Parkinson's disease associated protein DJ-1. ACS Chem Biol. 2018;13:2783–93.